Role of the $N^*(1440)$ resonance in the $pp \to pn\pi^+$ reaction

Zhen Ouyang [1,3,4)*], Ju-Jun Xie [2,3,4)†], Bing-Song Zou[2,3,4)‡], Hu-Shan Xu [1,3,4)§]

1) Institute of Modern Physics, CAS, Lanzhou 730000, China

2) Institute of High Energy Physics, CAS, Beijing 100049, China

3) Graduate University of Chinese Academy of Sciences, Beijing 100049, China

4) Theoretical Physics Center for Science Facilities, CAS, Beijing 100049, China

Abstract

New measurement by CELSIUS-WASA Collaboration on the $pp \to pn\pi^+$ reaction reveals clear evidence for the presence of the Roper resonance $N^*(1440)$ which has been ignored in previous theoretical calculations. In this article, based on an effective Lagrangian approach and available knowledge on the Roper resonance, we investigate the role of the Roper resonance for the $pp \to pn\pi^+$ reaction. It is found that the contribution from the Roper resonance $N^*(1440)$ becomes significant for kinetic energy above 1.1

*Corresponding author. ouyangzh@impcas.ac.cn; Tel: +86-10-88236162; fax: +86-10-88233085

†xiejujun@mail.ihep.ac.cn

‡zoubs@mail.ihep.ac.cn

§hushan@impcas.ac.cn

GeV, consistent with the new experimental observation. The t-channel σ-meson exchange is dominant for the production of the Roper resonance.

PACS: 13.75.Cs; 14.20.Gk; 13.30.Eg

keywords: *pp* collision; Pion production; $N^*(1440)$ resonance; Effective Lagrangian approach

1 Introduction

Ever since the first even-parity excited state of the nucleon, the Roper resonance $N^*(1440)$ was first deduced by πN phase shift analysis, its structure has been arousing people's interests intensely all the time—it is lighter than the first odd-parity nucleon excitation, the $S_{11}(1535)$, and also has a significant branching ratio into two pions. Up to now, although the existence of the Roper resonance is well established (4-star ranking in the particle data book), its properties, such as mass, width and decay branching ratios etc., still suffer large experiment uncertainties [1]. In classical quark models, the Roper resonance has been associated with the first spin-parity $J^P = 1/2^+$ radial excited state of the nucleon [2, 3, 4, 5]. In the bag model [6] and in the Skyrme model [7], a surface oscillation, also called breathing mode, has been predicted to interpret the Roper resonance as a monopole excitation of the nucleon. Furthermore, it has also been supposed to relate to a hybrid nature which means a gluonic excitation state of the nucleon [8, 9, 10]. The recent theoretical works [11, 12] found that the Roper resonance was dynamically generated from the meson-nucleon interactions. Nevertheless, the model predictions always reach either larger value for the Roper resonance mass or much smaller one for its width and also meet difficulties to explain its electromagnetic coupling [13].

In the early years, our knowledge on Roper resonance was mainly based on πN and γN experiments, however, it is excited so weakly thus buried by the strong Δ peak in these experiments. Another difficulty in extracting the Roper resonance information from these experiments is the isospin decomposition of 1/2 and 3/2 [14]. In Refs. [15, 16], it was pointed out that the decays of $J/\psi \to \bar{N}N\pi$ and $J/\psi \to \bar{N}N\pi\pi$ provide an ideal place for studying the properties of nucleon resonances, since in these processes the πN and $\pi\pi N$ systems are limited to be pure isospin-$\frac{1}{2}$ due to isospin conservation. The result from BES Collaboration on $J/\psi \to p\pi^-\bar{n}+$ c.c. reaction showed a clear N^* peak in the $N\pi$ invariant mass spectrum around 1360 MeV/c^2 which gave the first direct observation of the Roper resonance peak in the πN invariant mass spectrum [17]. Nevertheless, since the Roper resonance has a strong coupling to σN, studying the Roper resonance from other production processes, *i.e.*, $\sigma N \to N^*(1440)$, is necessary, as also suggested in Refs. [18, 19].

Recently, the CELSIUS-WASA Collaboration performed a measurement on the $pp \to pn\pi^+$ reaction with proton beam of kinetic energy $T_P = 1.3$ GeV. They also observed a clear resonance structure in the invariant $n\pi^+$ mass spectrum for the Roper resonance at $M \approx 1360$ MeV/c^2 with a width of about 150 MeV [20, 21]. These values agree well with the BES result [17] and the pole position of the Roper resonance from πN phase shift analyses [1]. The $pp \to pn\pi^+$ reaction has the largest cross section for pp collision in the intermediate energy region around $T_P = 1.3$ GeV. It can be further studied by WASA-at-COSY and HIRFL-CSR facilities with much higher precision and statistics. This reaction opens a new window for studying the Roper resonance.

However, up to now, theoretical study on this channel in the intermediate energy region is scarce. In Ref. [22], Engel *et al.* performed a fully covariant calculation for the total cross section of the $pp \to pn\pi^+$ reaction. However, unaware of the significant role of the Roper

resonance for this reaction, their calculations only included the Δ resonance and the off-shell nucleon pole. Furthermore, in their calculations they did not consider the final-state interaction of pn. In Ref. [23], the authors performed their calculations for $T_P = 0.8$ GeV by including only the Δ resonance.

Inspired by the new observation of the Roper resonance by the CELSIUS-WASA Collaboration [20, 21], here we investigate the role of the Roper resonance for the $pp \to pn\pi^+$ reaction, based on an effective Lagrangian approach and available knowledge on the Roper resonance.

In next section, we will give the formalism and ingredients for our calculation. Then numerical results and discussion are given in Sect.3.

2 Formalism and ingredients

We study the $pp \to pn\pi^+$ reaction in an effective Lagrangian approach. All the basic Feynman diagrams involved for the reaction are depicted in Fig. 1. The so-called "pre-emission" diagrams [22] are not shown. But their contributions are included in actual calculations. In addition to the $\Delta(1232)$ and the off-shell nucleon pole included in previous works [22, 23, 24, 25], the Roper resonance is added in our calculation. For the production of the Roper resonance and the intermediate virtual nucleon, the π^0 and σ-meson exchanges are included while the ρ-meson exchange is found to give negligible contribution and is dropped. For the production of the $\Delta(1232)$ resonance, we only include π-meson exchange since iso-scalar meson exchanges cannot contribute and according to Ref. [23] any attempt to include the ρ-meson exchange worsens the agreement with experiments of $pp \to n\Delta^{++}$ reactions. A Lorentz covariant orbital-spin(L-S) scheme [26] are used for the effective $\Delta\pi N$, $N^*\sigma N$, and $N^*\pi N$ vertices.

2.1 Meson-Baryon-Baryon (Resonances) vertices

The effective Lagrangian densities involved for describing the πNN and σNN vertices are,

$$\mathcal{L}_{\pi NN} = -\frac{f_{\pi NN}}{m_\pi}\overline{u}_N\gamma_5\gamma_\mu\vec{\tau}\cdot\partial^\mu\vec{\psi}_\pi u_N, \tag{1}$$

$$\mathcal{L}_{\sigma NN} = g_{\sigma NN}\overline{u}_N\psi_\sigma u_N. \tag{2}$$

At each vertex a relevant off-shell form factor is used. In our computation, we take the same form factors that used in the well-known Bonn potential model [27]:

$$F_M^{NN}(k_M^2) = \frac{\Lambda_M^2 - m_M^2}{\Lambda_M^2 - k_M^2}, \tag{3}$$

where k_M, m_M and Λ_M are the 4-momenta, mass and cut-off parameter for the exchanged meson (M), respectively. In the Bonn meson-exchange model [27] for the nucleon-nucleon interaction, $k_M^0 = 0$, hence $k_M^2 = -|\vec{k}_M|^2$ is negative. For the $pp \to \pi^+pn$, it can easily verify that for the t-channel meson exchange, the k_M^2 still keeps negative. Therefore the off-shell form factors here always give a suppression factor. The coupling constants and the cut-off parameters are taken as the following ones [27, 28, 29, 30, 31, 32]: $g_{\pi NN}^2/4\pi = 14.4$, $\Lambda_\pi = 1.3$ GeV, $g_{\sigma NN}^2/4\pi = 5.69$ and $\Lambda_\sigma = 1.7$ GeV. Note that the constant $g_{\pi NN}$ is related to $f_{\pi NN}$ of Eq. (1) as $g_{\pi NN} = (f_{\pi NN}/m_\pi)2m_N$ [33].

To calculate the amplitudes of diagrams in Fig. 1 with the resonance model, we also need to know interaction vertices involving $\Delta(1232)$ and $N^*(1440)$ resonances. In Ref. [26], a Lorentz covariant orbital-spin scheme for N^*NM couplings has been described in detail, which can be easily extended to describe the $\Delta(1232)N\pi$, $N^*(1440)N\pi$ and $N^*(1440)N\sigma$ couplings that appear in the Feynman diagrams depicted in Fig. 1. By using that scheme, we can easily

obtain the effective $\Delta(1232)N\pi$,$N^*(1440)N\pi$, and $N^*(1440)N\sigma$ couplings:

$$\mathcal{L}_{\pi N\Delta(1232)} = g_{\Delta(1232)N\pi}\overline{u}_N\partial^\mu\psi_\pi u_{\Delta(1232)\mu} + \text{h.c.}, \quad (4)$$

$$\mathcal{L}_{\pi NN^*(1440)} = g_{N^*(1440)N\pi}\overline{u}_N\gamma_5\gamma_\mu\partial^\mu\psi_\pi u_{N^*(1440)} + \text{h.c.}, \quad (5)$$

$$\mathcal{L}_{\sigma NN^*(1440)} = g_{N^*(1440)N\sigma}\overline{u}_N\psi_\sigma u_{N^*(1440)} + \text{h.c.}, \quad (6)$$

with u_N, $u_{N^*(1440)}$, $u_{\Delta^*\mu}$, ψ_π, and ψ_σ as the wave functions for the nucleon, $N^*(1440)$ resonance, $\Delta^*(1232)$ resonance, π and σ-meson, respectively.

For the relevant vertices involving $\Delta(1232)$ and $N^*(1440)$ resonances, the off-shell form factors are adopted as below:

$$F_M(k_M^2) = (\frac{\Lambda_M^{*2} - m_M^2}{\Lambda_M^{*2} - k_M^2})^n, \quad (7)$$

where n=1 for the Roper resonance and n=2 for the $\Delta(1232)$ resonance [18, 22, 34], with Λ_M^* being the corresponding cut-off parameters which are: $\Lambda_\pi^\Delta = 0.59$ GeV, $\Lambda_\pi^{N^*(1440)} = 1.3$ GeV [18] and $\Lambda_\sigma^{N^*(1440)} = 1.5$ GeV [34]. Here a quite severe cutoff Λ_π^Δ is needed to reproduce data, in consistent with the previous study [23] of $pp \to n\Delta^{++}$ reactions.

It is worth noting that we also take the virtuality of the intermediate nucleon into account by introducing a form factor which is taken as in Refs. [35, 36, 37]

$$F(q) = \frac{\Lambda_N^4}{\Lambda_N^4 + (q^2 - m_N^2)^2}, \quad (8)$$

with Λ_N= 0.6 GeV.

2.2 Coupling constants for the intermediate resonances

The $\Delta(1232)N\pi$ and $N^*(1440)N\pi$ coupling constants are determined from the experimentally observed partial decay widths of the Δ and Roper resonances. The general formula for the partial decay width of $\Delta(1232)$ or $N^*(1440)$ resonance decaying into a nucleon and a pion is as

the following

$$d\Gamma = \overline{|\mathcal{M}_{R\to N\pi}|^2}(2\pi)^4\delta^4(q_R - p_N - p_\pi)\frac{d^3p_N}{(2\pi)^3}\frac{m_N}{E_N}\frac{d^3p_\pi}{(2\pi)^3}\frac{1}{2E_\pi}, \tag{9}$$

where $\mathcal{M}_{R\to N\pi}$ stands for the total amplitude of the initial resonance decaying to a nucleon and a pion, the q_R, p_N and p_π are the 4-momenta of the three particles, E_N and E_π are the corresponding energies. With the effective Lagrangians described by Eq. (4) and Eq. (5), the partial decay widths can be calculated

$$\Gamma_{N^*(1440)\to N\pi} = \frac{3g^2_{N^*(1440)N\pi}p_N^{cm}}{4\pi}[\frac{m_\pi^2(E_N - m_N)}{M_{N^*(1440)}} + 2(p_N^{cm})^2] \tag{10}$$

with

$$p_N^{cm} = \sqrt{\frac{(M^2_{N^*(1440)} - (m_N + m_\pi)^2)(M^2_{N^*(1440)} - (m_N - m_\pi)^2)}{4M^2_{N^*(1440)}}}, \tag{11}$$

$$E_N = \sqrt{(p_N^{cm})^2 + m_N^2}, \tag{12}$$

$$\Gamma_{\Delta^*(1232)N\pi} = \frac{g^2_{\Delta^*(1232)N\pi}(m_N + E_N)(p_N^{cm})^3}{12\pi M_{\Delta^*(1232)}}, \tag{13}$$

with p_N^{cm} here the momentum of the nucleon in the rest frame of $\Delta(1232)$.

For the $N^*(1440)N\sigma$ coupling constant, we get it from the partial decay width of $N^*(1440) \to N\sigma \to N\pi\pi$, which is given by

$$d\Gamma_{N^*(1440)\to N\sigma\to N\pi\pi} = \overline{|\mathcal{M}_{N^*\to N\sigma\to N\pi\pi}|^2}\frac{d^3p_1}{(2\pi)^3}\frac{m_1}{E_1}\frac{d^3p_2}{(2\pi)^3}\frac{1}{2E_2}\frac{d^3p_3}{(2\pi)^3}\frac{1}{2E_3}(2\pi)^4\delta^4(p_{N^*} - p_1 - p_2 - p_3) \tag{14}$$

with

$$\mathcal{M}_{N^*\to N\sigma\to N\pi\pi} = 2g_{\pi\pi\sigma}g_{N^*N\sigma}F_\sigma^{N^*N}(k_\sigma^2)\bar{u}_N(p_1, s_1)\frac{i}{k_\sigma^2 - m_\sigma^2 + im_\sigma\Gamma_\sigma}p_2\cdot p_3\bar{u}_{N^*}(p_{N^*}, s_{N^*}), \tag{15}$$

where $\mathcal{M}_{N^*\to N\sigma\to N\pi\pi}$ represents the total amplitude of $N^*(1440) \to N\sigma \to N\pi\pi$. p_{N^*} and k_σ denote the 4-momenta of the $N^*(1440)$ resonance and the intermediate σ meson; m_σ and Γ_σ

are the mass and full width of the σ meson, which we take $m_\sigma = 550$ MeV and $\Gamma_\sigma = 500$ MeV; p_1, m_1, and E_1 stand for the 4-momenta, mass, and energy of the nucleon; s_1 and s_{N^*} the spin projection of the nucleon and the $N^*(1440)$ resonance; p_2, p_3, and E_2, E_3 stand for the 4-momenta and energy of the final two pions, respectively. To calculate the amplitude of $\sigma \to \pi\pi$ appearing in the total amplitude calculation, we use the following type of vertex

$$\mathcal{L}_{\pi\pi\sigma} = g_{\pi\pi\sigma}\partial_\mu\vec{\psi}_\pi \cdot \partial^\mu\vec{\psi}_\pi\psi_\sigma, \tag{16}$$

where the coupling constant $g_{\pi\pi\sigma}$ can be determined from the partial decay width $\Gamma_{\sigma\to\pi\pi}$

$$d\Gamma_{\sigma\to\pi\pi} = \frac{1}{2m_\sigma}\overline{|\mathcal{M}_{\sigma\to\pi\pi}|^2}\frac{d^3p_1}{(2\pi)^3}\frac{1}{2E_1}\frac{d^3p_2}{(2\pi)^3}\frac{1}{2E_2}(2\pi)^4\delta^4(p_\sigma - p_1 - p_2), \tag{17}$$

where $\mathcal{M}_{\sigma\to\pi\pi}$ represents the total amplitude of $\sigma \to \pi\pi$. p_1, p_2, and E_1, E_2 stand for the 4-momenta and energy of the final two pions, respectively.

With the experimental branching ratios [1] and the above formulae, we obtain all the corresponding coupling constants as summarized in Table 1.

2.3 Propagators

In our amplitude calculation of Feynman diagrams in Fig. 1, we also need propagators for the π and σ-meson, and the intermediate $\Delta(1232)$ and $N^*(1440)$ resonances with half-integer spin as well. For the π and σ-meson, the propagators are

$$G_{\pi/\sigma}(k_{\pi/\sigma}) = \frac{i}{k^2_{\pi/\sigma} - m^2_{\pi/\sigma}}, \tag{18}$$

where $k_{\pi/\sigma}$ are the 4-momenta of π and σ-meson, respectively; $m_{\pi/\sigma}$ are their corresponding masses.

The propagators for the $\Delta(1232)$ and $N^*(1440)$ resonances can be constructed with their projection operators and the corresponding Breit-Wigner factor [38]. The spin-(n+$\frac{1}{2}$) resonance

propagator can be written as

$$G^{n+\frac{1}{2}}(q) = P^{(n+\frac{1}{2})}\frac{2M_R}{q^2 - M_R^2 + iM_R\Gamma_R}, \tag{19}$$

where $1/(q^2 - M_R^2 + iM_R\Gamma_R)$ is the standard Breit-Wigner factor; M_R, q and Γ_R are the mass, four momentum and full width of the resonance, respectively. $P^{(n+\frac{1}{2})}$ is the projection operator

$$P^{\frac{1}{2}}(q) = \frac{\not{q} + M_R}{2M_R}, \tag{20}$$

$$P^{\frac{3}{2}}_{\mu\nu}(q) = \frac{(\not{q} + M_R)}{2M_R}\left[g_{\mu\nu} - \frac{1}{3}\gamma_\mu\gamma_\nu - \frac{1}{3M_R}(\gamma_\mu q_\nu - \gamma_\nu q_\mu) - \frac{2}{3M_R^2}q_\mu q_\nu\right]. \tag{21}$$

With the projection operators, the propagators for the intermediate $\Delta(1232)(\frac{3}{2}^+)$ and $N^*(1440)(\frac{1}{2}^+)$ resonances can be easily obtained as the following

$$G^{N^*(1440)}(q) = \frac{\not{q} + M_{N^*(1440)}}{q^2 - M^2_{N^*(1440)} + iM_{N^*(1440)}\Gamma_{N^*(1440)}}, \tag{22}$$

$$G^{\Delta(1232)}_{\mu\nu}(q) = \frac{P_{\mu\nu}(q)}{q^2 - M^2_{\Delta(1232)} + iM_{\Delta(1232)}\Gamma_{\Delta(1232)}} \tag{23}$$

with

$$P_{\mu\nu}(q) \;\; = \;\; (\not{q} + M_{\Delta(1232)})[g_{\mu\nu} - \frac{1}{3}\gamma_\mu\gamma_\nu - \frac{\gamma_\mu q_\nu - \gamma_\nu q_\mu}{3M_{\Delta(1232)}} - \frac{2}{3M^2_{\Delta(1232)}}q_\mu q_\nu]. \tag{24}$$

For simplicity we use constant width in the Breit-Wigner (BW) formula. The mass and width appearing in such constant-width BW formula are very close to their corresponding pole positions. In some detailed data fitting works, various energy dependent widthes are used in the BW formula. The mass and width appearing in such BW formula could then be very different from their corresponding pole positions. Usually the pole positions are better determined than the model dependent BW mass and width. For example, the BW mass and width given by PDG [1] with energy dependent width are (1420 $\sim$ 1470) MeV and (200 $\sim$ 450) MeV, respectively; while the corresponding pole positions listed in PDG [1] are (1350 $\sim$ 1380) MeV

and (160 $\sim$ 220) MeV, respectively. Hence, for parameters appearing in the constant-width BW propagators, we adopt $M_{\Delta(1232)} = 1.21$ GeV, $\Gamma_{\Delta(1232)} = 100$ MeV, $M_{N^*(1440)} = 1.365$ GeV and $\Gamma_{N^*(1440)} = 190$ MeV, as given by PDG for their corresponding pole positions [1].

As for the intermediate virtual nucleon, we use

$$G^N(q) = \frac{\not{q} + m_N}{q^2 - m_N^2} \tag{25}$$

as its propagator, with M_N and q being the mass and 4-momenta of the virtual nucleon, respectively.

2.4 Amplitude and total cross section for $pp \to pn\pi^+$ reaction

In order to show the structure of total amplitude in terms of the meson exchange and the intermediate resonances, we write down explicitly the total amplitude in our calculation for the $pp \to pn\pi^+$ reaction as the sum of sub-amplitudes

$$\begin{aligned} \mathcal{M} &= \mathcal{M}(\Delta(1232), \pi^+) + \mathcal{M}(\Delta(1232), \pi^0) + \mathcal{M}(N^*(1440), \pi^0) + \mathcal{M}(N^*(1440), \sigma) + \\ &\quad \mathcal{M}(p(938), \pi^0) + \mathcal{M}(p(938), \sigma), \end{aligned} \tag{26}$$

where on the right-hand side of the equation, the resonances and mesons exchanged in the intermediate states are written inside the bracket explicitly. Each sub-amplitude can be obtained straightforwardly with effective couplings and propagators given in former sections by following the Feynman rules. The explicit expressions of the amplitudes are given in Appendix.

For the final-state-interaction(FSI) between the three outgoing particles, we only need to consider p-n FSI enhancement factor near threshold, since the interaction between $n\pi^+$ and $p\pi^+$ are dominated by the s-channel intermediate resonances. To study possible influence from the p-n final state interaction, we include it in our calculation by factorizing the reaction amplitude

as

$$\mathcal{A} = \mathcal{M}(pp \to pn\pi^+) T_{pn}, \tag{27}$$

where $\mathcal{M}(pp \to pn\pi^+)$ is the primary production amplitude as discussed above, T_{pn} describes the p-n final state interaction, which goes to unity in the limit of no FSI. The enhancement factor T_{pn} is taken into account by means of the general framework based on the Jost function formalism [39, 40] with

$$T_{pn} = \frac{k + i\beta}{k - i\alpha}. \tag{28}$$

where k is the internal momentum of p-n subsystem, and the α and β are associated with the effective-range parameters via [41]

$$\alpha = \frac{1}{r}(1 - \sqrt{1 - \frac{2r}{a}}), \qquad \beta = \frac{1}{r}(1 + \sqrt{1 - \frac{2r}{a}}). \tag{29}$$

According to the FSI analysis of Ref. [41] on the reaction $pp \to pn\pi^+$ at the beam energy of $T_p = 0.95$ GeV, the triplet $^3S_1$ np state dominates the np invariant mass spectrum at the low mass end with negligible singlet $^1S_0$ state contribution. So in the present work, we assume the total amplitude with triplet $^3S_1$ np state dominating the np near threshold region, and multiply the total amplitude with the FSI factor of triplet $^3S_1$ np state with the parameters adopted from Ref. [41], *i.e.*,

$$a_t = 5.424 \ \text{ fm}, \qquad r_t = 1.759 \ \text{ fm}. \tag{30}$$

Then the calculation of the invariant amplitude square $|\mathcal{A}|^2$ and the cross section $\sigma(pp \to pn\pi^+)$ are straightforward,

$$d\sigma(pp \to pn\pi^+) = \frac{1}{4}\frac{m_p^2}{F}\sum_{s_i}\sum_{s_f}|\mathcal{A}|^2 \frac{m_p d^3p_3}{E_3}\frac{d^3p_\pi}{2E_\pi}\frac{m_n d^3p_n}{E_n}\delta^4(p_1 + p_2 - p_3 - p_\pi - p_n), \tag{31}$$

with the flux factor

$$F = (2\pi)^5 \sqrt{(p_1 \cdot p_2)^2 - m_p^4}. \tag{32}$$

The factors 1/4 and $\sum_{s_i} \sum_{s_f}$ emerge for the simple reason that the polarization of initial and final particles is not considered. Since the relative phases among various meson exchanges in the amplitude of Eq. (26) are unknown, the interference terms are ignored in our concrete calculations.

In the amplitude given above, we have neglected the pp initial-state-interaction (ISI) factor which has been used by many authors in investigating $pp \to pp\eta$ reaction [42, 43]. The role of the ISI in the production of a heavy meson from an NN collision is basically to reduce the cross section near threshold by an overall factor with little energy dependence, although with some controversy about its absolute value. While the ISI factor with $pp \to pp\eta$ reaction near threshold is relatively simple with ${}^3P_0$ pp initial state dominant, it becomes technically more complicated for $pp \to NN\pi$ with several important initial partial waves even at energies very close to the threshold. In practice, for the pion production reactions, the ISI dumping effect is not included explicitly in previous calculations [22, 23] and is done by adjusting the vertex form factors to reproduce the total cross sections. Since how to treat this dumping factor does not influence our main conclusion here, we follow the simple practical approach as these previous calculations [22, 23] on the same reaction, although the ISI could be taken into account by some more complicated approaches, such as by including the partial wave ISI factors [42, 43] or distortions of wave functions [44, 45, 46].

3 Numerical results and discussion

With the formalism and ingredients discussed in the former sections, we evaluated the total cross section versus the kinetic energy of the proton beam (T_P) for the $pp \to pn\pi^+$ reaction by using the code FOWL from the CERN program library, which is a program for Monte Carlo multi-particle phase space integration weighted by the amplitude squared. The results for T_P ranging from 0.2 to 1.3 GeV are shown in Fig. 2 and Fig. 3 along with experimental data [47, 48] for comparison.

In Fig. 2, the results obtained from with and without including the $^3S_1$ np FSI factor are represented by solid and dashed curves, respectively. We can see our theoretical result without FSI agrees well with the experimental data at beam energies near 1.0 GeV. However, at lower beam energies,the calculated total cross sections underestimate the data by a factor of 4 or more. In view of the important role of FSI for the near-threshold enhancement, we also tried to include it and found that the result with FSI is indeed in excellent agreement with the experimental data over a wide range of beam energies. Both the energy dependence and the absolute magnitudes of the experimental data are very well reproduced. Note that in reality, the np $^3S_1$ partial wave should dominate only at energies close to threshold. For energies of a few hundred MeV above threshold, the contributions from higher partial waves become important. The FSI effect due to the strong np $^3S_1$ interaction should become less important as energy increases. Hence after taking this effect into account, one would expect to get theoretical results closer to the solid curve at low energies and to the dashed curve at higher energies in the Fig. 2.

In Fig. 3, individual contributions corresponding to $\Delta(1232)$ with π^+ and π^0 exchange, $N^*(1440)$ with σ and π^0 exchange, and nucleon pole with σ and π^0 exchange are shown in

comparison with the experimental data by dotted, short-dotted, dot-dashed, dot-dot-dashed, dashed, and short-dashed curves, respectively. The contribution from the $\Delta^{++}(1232)$ production by the π^+ exchange is found to be dominant for T_P between 0.6 and 1.1 GeV. The $\Delta^+(1232)$ with π^0 exchange gives one order of magnitude smaller contribution for the cross section than $\Delta^{++}(1232)$ with π^+ exchange over the whole energy region, simply due to smaller isospin factor of 1/9. In Ref. [23], by only including the contribution of the $\Delta(1232)$ resonance the authors reproduced the experimental points for present channel fairly well, however, visibly underestimated the data points close to threshold. Actually, from Fig. 3, one can see that the nucleon pole by σ meson exchange plays a more important role for beam energies close to threshold. This is consistent with the previous calculation for the $pp \to pp\pi^0$ reaction [45], where it is shown that the prediction with only pion exchange [46] underestimates the data by a factor about 5. And there are more examples from other reactions showing the significance of the sub-threshold nucleon pole contribution, such as in $J/\psi \to \bar{p}n\pi^+$ [17, 49]. In contrast, contribution of the nucleon pole by π^0 exchange is much smaller than by σ exchange over the whole energy region. Furthermore, it is worth noting that contribution of the $N^*(1440)$ resonance by σ exchange becomes quite significant at beam energies above 1.1 GeV, larger than all other contributions except $\Delta^{++}(1232)$ contribution, though it is negligibly small at lower beam energies. The contribution of the $N^*(1440)$ by π^0 exchange is much smaller by a factor of about 10 or more, which indicates that by no means can it account for the clear Roper peak in the invariant mass $M_{n\pi^+}$ spectrum. Anyway, the σ-meson exchange is found to play a significant role, which has also been pointed out in a previous study of αp reaction [18]. Possible contribution from the neighborhood $N^*(1535)$ resonance is also checked and is found to be negligible in the present energy region.

In our present calculation, we have not included the contribution from πN S-wave re-

scattering process, which was found to be the dominant production mechanism for the π^+ production at the energies very close to the threshold [50]. Since the main interests of the present work is for the N^* production at higher energies and in our approach the uncertainties from FSI and ISI are also quite large at the energies very close to the threshold, we refer the readers who are interested in the very near threshold regime to the more dedicated study of this regime by Ref. [50].

In our concrete calculation, the interference terms between various resonances are ignored because the relative phases from various resonances are unknown. In order to get some feeling about the importance of the interference terms, we calculated the magnitudes of a few largest ones. At the high energy end $T_P = 1.3$ GeV, the largest two contributions come from Δ^{++} and $N^*(1440)$ resonances as shown in Fig. 3. For the cross section, the contribution of the interference term from these two resonances is found to be in the range of $\pm 5\%$ of the contribution from the Δ^{++} resonance alone. At the lower energies around 0.4 GeV, the largest two contributions from Δ^{++} and off-shell nucleon are comparable, but the contribution from their interference term is found to be only around $\pm 1\%$ to the total cross section by integrating over the whole three-body phase space.

The invariant mass spectra and Dalitz plot for the final particles of $pp \to pn\pi^+$ reaction at $\mathrm{T_P} = 1.3$ GeV are also calculated as shown in Fig.4. While the $\Delta^{++}(1232)$ peak dominates the $p\pi^+$ invariant mass spectrum, a peak due to $N^*(1440)$ is clearly visible in the $n\pi^+$ invariant mass spectrum. As a rough comparison with data, preliminary results with two different triggers and without proper acceptance correction from CELSIUS-WASA Collaboration [20, 21] are also shown in the $p\pi^+$ and $n\pi^+$ invariant mass spectra. Individual contributions to the invariant mass spectra from $\Delta(1232)$, $N^*(1440)$ and nucleon pole are also given in Fig. 4 by dashed, dotted, and dot-dashed curves, respectively. From the $n\pi^+$ invariant mass spectrum, one can

see that the reflection of $\Delta^{++}(1232)$ resonance gives a large but flat contribution, the isospin suppressed $\Delta^{+}(1232)$ contribution gives a weak peak around 1.23 GeV, and the Roper $N^{*}(1440)$ resonance is absolutely needed to reproduce the peak around 1.36 GeV. In the calculation for $T_P = 1.3$ GeV, the n-p FSI factor is not included since the data for both $p\pi^+$ and $n\pi^+$ mass spectra have no evidence for the FSI effect which should cause further enhancement for both mass spectra at high energy end. The phenomena may suggest that at beam energy about 1.3 GeV the contribution from p-n higher partial waves has already exceeded the $^3S_1$ partial wave to be the dominant contribution and the S-wave FSI becomes unimportant. The forthcoming acceptance corrected results from the CELSIUS-WASA Collaboration and future experiments at COSY with the newly installed WASA-at-COSY detector [51] or at HIRFL-CSR with the scheduled 4π hadron detector [52] will be very helpful for constraining the ingredients in our model calculations.

In our calculation, the only free parameter we adjust is the Λ_π^Δ for the $\Delta\pi N$ vertex form factor. Previous calculations used $\Lambda_\pi^\Delta = 0.65$ GeV [23] and 0.63 GeV [53]. Whereas they included only the Δ resonance to reproduce the total cross sections for the $pp \to pn\pi^+$ reaction, we need to reduce it to 0.59 GeV to allow contributions from the off-shell nucleon pole and the Roper resonance for the best description of the total cross section.

The experimental study [20, 21] and our theoretical study here suggest that the $pp \to pn\pi^+$ reaction provides a very good place for studying the N^* resonances. Since all the contributions from Δ^{*+} resonances are well constrained by the corresponding Δ^{*++} contributions by an isospin scaling factor of 1/9 and hence suppressed, the $n\pi^+$ invariant mass spectrum for this reaction provides a rather good isospin filter for N^* resonant peaks. Therefore the study of this reaction should be extended to higher energies at COSY and HIRFL-CSR with 4π detectors to provide various differential cross sections and the Dalitz plot. It will definitely help us to look

for those "missing" Δ^{*++} resonances with large coupling to $\rho^+ p$ and N^* resonances with large coupling to $N\sigma$ or $N\omega$ at higher energies. The information on various couplings of observed Δ^* and N^* resonances may also help us gain some insight on the nature of these resonances [32].

Acknowledgements: We would like to thank H. Clement, B.C. Liu and J.J. Wu for useful discussions. This work is partly supported by the National Natural Science Foundation of China under grants Nos. 10435080, 10521003, 10875133, 10635080, and by the Chinese Academy of Sciences under projects Nos. KJCX2-SW-N18, KJCX3-SYW-N2, CXTD-J2005-1.

References

[1] C. Amsler et al. (PDG Collaboration), Phys. Lett. B667 (2008) 1.

[2] N. Isgur and G. Karl, Phys. Rev. D18 (1978) 4187;
N. Isgur and G. Karl, Phys. Rev. D19 (1979) 2653.

[3] S. Capstick and N. Isgur, Phys. Rev. D34 (1986) 2809.

[4] L.Y. Glozman et al., Phys. Rev. D58 (1998) 094030.

[5] K.F. Liu and C.W. Wong, Phys. Rev. D28 (1983) 170.

[6] U.G. Meißner and J.W. Durso, Nucl. Phys. A430 (1984) 670.

[7] C. Hajduk and B. Schwesinger, Phys. Lett. B140 (1984) 172.

[8] T. Barnes and F.E. Close, Phys. Lett. B123 (1983) 89.

[9] E. Golowich, E. Haqq and G. Karl, Phys. Rev. D28 (1983) 160.

[10] L. Kisslinger and Z.P. Li, Phys. Rev. D51 (1995) R5986.

[11] O. Krehl et al., Phys. Rev. C62 (2000) 025207.

[12] C. Schütz, J. Haidenbauer, J. Speth and J.W. Durso, Phys. Rev. C57 (1998) 1464.

[13] A.V. Sarantsev et al. (CB-ELSA and A2-TAPS Collaborations), Phys. Lett. B659 (2008) 94.

[14] R. Workman, Few Body Syst. Suppl. 11 (1999) 94.

[15] B.S. Zou, Nucl. Phys. A675 (2000) 167;
B.S. Zou, Nucl. Phys. A684 (2001) 330.

[16] B.S. Zou et al., Eur. Phys. J. A11 (2001) 341.

[17] M. Ablikim et al. (BES Collaboration), Phys. Rev. Lett. 97 (2006) 062001.

[18] S. Hirenzaki, P. Fernández de Córdoba and E. Oset, Phys. Rev. C53 (1996) 277.

[19] L. Alvarez-Ruso, E.Oset and E. Hernández, Nucl. Phys. A633 (1998) 519.

[20] H. Clement et al. (CELSIUS-WASA Collaboration), Evidence for a 'Narrow' Roper Resonance - The Breathing Mode of the Nucleon, nucl-ex/0612015.

[21] H. Clement, Talk at NSTAR2007, Bonn, Germany, September 2007.

[22] A. Engel, R. Shyam, U. Mosel and A.K. Dutt-Mazumder, Nucl. Phys. A603 (1996) 387.

[23] B. Kundu, B.K. Jain and A.B. Santra, Phys. Rev. C58 (1998) 1614.

[24] J. Hudomalj-Gabitzsch et al., Phys. Rev. C18 (1978) 2666.

[25] R. Shyam and U. Mosel, Phys. Lett. B426 (1998) 1.

[26] B.S. Zou and F. Hussain, Phys. Rev. C67 (2003) 015204.

[27] R. Machleidt, K. Holinde and Ch. Elster, Phys. Rep. 149 (1987) 1;

R. Machleidt, Adv. Nucl. Phys. 19 (1989) 189.

[28] K. Tsushima, S.W. Huang and A. Faessler, Phys. Lett. B337 (1994) 245;

K. Tsushima, S.W. Huang and A. Faessler, J. Phys. G21 (1995) 33.

[29] K. Tsushima, A. Sibirtsev and A.W. Thomas, Phys. Lett. B390 (1997) 29.

[30] K. Tsushima et al., Phys. Rev. C59 (1999) 369;

K. Tsushima et al., Phys. Rev. C61 (2000) 029903, Erratum.

[31] A. Sibirtsev, K. Tsushima, W. Cassing and A.W. Thomas, Nucl. Phys. A646 (1999) 427.

[32] J.J. Xie and B.S. Zou, Phys. Lett. B649 (2007) 405;

J.J. Xie, B.S. Zou and H.C. Chiang, Phys. Rev. C77 (2008) 015206.

[33] M.D. Scadron, Advanced Quantum Theory and Its Applications through Feynman Diagrams (Springer-Verlag, New York, 1979) p.228.

[34] E. Hernández and E. Oset, Phys. Rev. C60 (1999) 025204.

[35] G. Penner and Mosel, Phys. Rev. C66 (2002) 055211;

G. Penner and Mosel, Phys. Rev. C66 (2002) 055212.

[36] V. Shklyar, H. Lenske and U. Mosel, Phys. Rev. C72 (2005) 015210.

[37] T. Feuster and U. Mosel, Phys. Rev. C58 (1998) 457;

T. Feuster and U. Mosel, Phys. Rev. C59 (1999) 460.

[38] W.H. Liang, P.N. Shen, J.X. Wang and B.S. Zou, J. Phys. G28 (2002) 333.

[39] J. Gillespie, Final-State Interaction (Holden-Day, San Francisco, 1964).

[40] M.L. Goldberger and K.M. Watson, Collision Theory (John Wiley and Sons, New York, 1964).

[41] F. Hinterberger, S.N. Nedev and R. Siudak, Int. J. Mod. Phys. A20 (2005) 291.

[42] C. Hanhart and K. Nakayama, Phys. Lett. B454 (1999) 176; K. Nakayama, J. Speth, and T.S.H. Lee, Phys. Rev. **C65** (2002) 045210; K. Nakayama, J.W. Durso, J. Haidenbauer, C.Hanhart and J. Speth, Phys. Rev. C 60 (1999) 055209.

[43] G. Fäldt and C. Wilkin, Phys. Scripta 64 (2001) 427.

[44] V. Baru et al., Phys. Rev. C67 (2003) 024002.

[45] C.J. Horowitz, H.O. Meyer and D.K. Griegel, Phys. Rev. C49 (1994) 1337.

[46] D. S. Koltun and A. Reitan, Phys. Rev. 141 (1966) 1413.

[47] A. Baldini, V. Flamino, W.G. Moorhead and D.R.O. Morrison, Landolt-Börnstein, Numerical Data and Functional Relationships in Science and Technology, Vol. 12, Total Cross Sections for Reactions of High Energy Particles, ed. by H. Schopper (Springer-Verlag, Berlin, 1988).

[48] J.G. Hardie et al., Phys. Rev. C56 (1997) 20.

[49] W.H. Liang et al., Eur. Phys. J. A21 (2004) 487.

[50] V. Lensky, V. Baru, J. Haidenbauer, C. Hanhart, A. E. Kudryavtsev and U. G. Meissner, Eur. Phys. J. A **27** (2006) 37.

[51] H.-H. Adam et al. (WASA-at-COSY Collaboration), Proposal for the Wide Angle Shower Apparatus (WASA) at COSY-Jülich, nucl-ex/0411038.

[52] W.L. Zhan, Talk at MENU2004, Beijing, China, August 2004;

H.S. Xu, Talk at the Workshop on hadron physics at COSY and CSR, Lanzhou, China, January 2006.

[53] V. Dmitriev, O. Sushkov and C. Gaarde, Nucl. Phys. A459 (1986) 503.

Appendix

In this appendix we present explicitly the expression of each amplitude in our calculation of Eq.(26) as the following:

$$\mathcal{M}(\Delta(1232),\pi^+) = \sqrt{2}\frac{f_{\pi NN}}{m_\pi} g^2_{\Delta N\pi} F^{NN}_\pi(k^2_\pi) F^{\Delta N}_\pi(k^2_\pi) \bar{u}_3(p_3,s_3) p^\nu_\pi G^{\Delta(1232)}_{\nu\mu}(q) k^\mu_\pi u_1(p_1,s_1)$$
$$G_\pi(k_\pi)\bar{u}_n(p_n,s_n)\gamma_5 \not{k}_\pi u_2(p_2,s_2) - (\text{exchange term with } p_1 \leftrightarrow p_2), \quad (33)$$

$$\mathcal{M}(\Delta(1232),\pi^0) = \frac{\sqrt{2}}{3}\frac{f_{\pi NN}}{m_\pi} g^2_{\Delta N\pi} F^{NN}_\pi(k^2_\pi) F^{\Delta N}_\pi(k^2_\pi) \bar{u}_n(p_n,s_n) p^\nu_\pi G^{\Delta(1232)}_{\nu\mu}(q) k^\mu_\pi u_1(p_1,s_1)$$
$$G_\pi(k_\pi)\bar{u}_3(p_3,s_3)\gamma_5 \not{k}_\pi u_2(p_2,s_2) - (\text{exchange term with } p_1 \leftrightarrow p_2), \quad (34)$$

$$\mathcal{M}(N^*(1440),\pi^0) = \sqrt{2}\frac{f_{\pi NN}}{m_\pi} g^2_{N^*N\pi} F^{NN}_\pi(k^2_\pi) F^{N^*N}_\pi(k^2_\pi) \bar{u}_n(p_n,s_n)\gamma_5 \not{p}_\pi G^{N^*(1440)}(q)\gamma_5 \not{k}_\pi u_1(p_1,s_1)$$
$$G_\pi(k_\pi)\bar{u}_3(p_3,s_3)\gamma_5 \not{k}_\pi u_2(p_2,s_2) - (\text{exchange term with } p_1 \leftrightarrow p_2), \quad (35)$$

$$\mathcal{M}(N^*(1440),\sigma) = \sqrt{2} g_{\sigma NN} g_{N^*N\sigma} g_{N^*N\pi} F^{NN}_\sigma(k^2_\sigma) F^{N^*N}_\sigma(k^2_\sigma) \bar{u}_n(p_n,s_n)\gamma_5 \not{p}_\pi G^{N^*(1440)}(q) u_1(p_1,s_1)$$
$$G_\sigma(k_\sigma)\bar{u}_3(p_3,s_3) u_2(p_2,s_2) - (\text{exchange term with } p_1 \leftrightarrow p_2), \quad (36)$$

$$\mathcal{M}(p(938),\pi^0) = \sqrt{2}(\frac{f_{\pi NN}}{m_\pi})^3 (F^{NN}_\pi(k^2_\pi))^2 F(q) \bar{u}_n(p_n,s_n)\gamma_5 \not{p}_\pi G^N(q)\gamma_5 \not{k}_\pi u_1(p_1,s_1)$$
$$G_\pi(k_\pi)\bar{u}_3(p_3,s_3)\gamma_5 \not{k}_\pi u_2(p_2,s_2) - (\text{exchange term with } p_1 \leftrightarrow p_2), \quad (37)$$

$$\mathcal{M}(p(938),\sigma) = \sqrt{2}\frac{f_{\pi NN}}{m_\pi} g^2_{\sigma NN} (F^{NN}_\sigma(k^2_\sigma))^2 F(q) \bar{u}_n(p_n,s_n)\gamma_5 \not{p}_\pi G^N(q) u_1(p_1,s_1)$$
$$G_\sigma(k_\sigma)\bar{u}_3(p_3,s_3) u_2(p_2,s_2) - (\text{exchange term with } p_1 \leftrightarrow p_2) \quad (38)$$

with $u_n(p_n,s_n)$, $u_3(p_3,s_3)$, $u_1(p_1,s_1)$, $u_2(p_2,s_2)$ the spin wave functions of the outgoing neutron, proton in the final state and two initial protons, respectively. p_π and $k_{\pi(\sigma)}$ stand for the 4-momenta of the outgoing π-meson and the exchanged $\pi(\sigma)$-meson, respectively. p_1 and p_2 represent the 4-momenta of the two initial protons.

The amplitudes corresponding to the "pre-emission" graphs are not given here, but are included in actual calculations. With these amplitudes, the $\sum_{s_i}\sum_{s_f}|\mathcal{A}|^2$ in Eq.(31) is computed with the standard MATHEMATICA package.

Table 1: Relevant paramters of $\Delta(1232)$ and $N^*(1440)$.

Figure 1: Feynman diagrams for $pp \to pn\pi^+$ reaction. Note that there are also the pre-emission counter parts of these diagrams where pion is emitted before collision. These graphs are not shown here, but included in the calculations.

Figure 2: Total cross section vs T_P for the $pp \to pn\pi^+$ reaction from our calculation compared with data [47, 48]. The solid and dashed lines represent the results with and without $^3S_1$ np FSI, respectively.

Figure 3: Contributions of various components and their simple incoherent sum as a function of T_P for the $pp \to pn\pi^+$ reaction compared with data [47, 48], without including np FSI. The dotted, short-dotted, dot-dashed, dot-dot-dashed, dashed, and short-dashed curves represent contributions from $\Delta(1232)(\pi^+$ and π^0 exchange), $N^*(1440)(\sigma$ and π^0 exchange) and nucleon pole (σ and π^0 exchange), respectively; the solid curve represents their simple incoherent sum.

Figure 4: Invariant mass spectra and Dalitz plot for the $pp \to pn\pi^+$ reaction at T_P = 1.3 GeV, compared with the preliminary data with two different triggers and without proper acceptance correction (open circles from Ref.[20] and solid circles from Ref.[21] with arbitrary normalization). The dashed, dotted and dot-dashed lines stand for individual contributions from $\Delta(1232)$, $N^*(1440)$ and nucleon pole, respectively, while the solid line represents their simple incoherent sum. In the Dalitz plot, the size of the squares indicates the magnitude of the number of events.

Table 1:

Resonances	Width(MeV)	Decay Channel	Branching ratios(%)	$g^2/4\pi$
$\Delta^*(1232)$	118	πN	100	19.54
$N^*(1440)$	300	πN	65	0.51
		σN	7.5	2.84

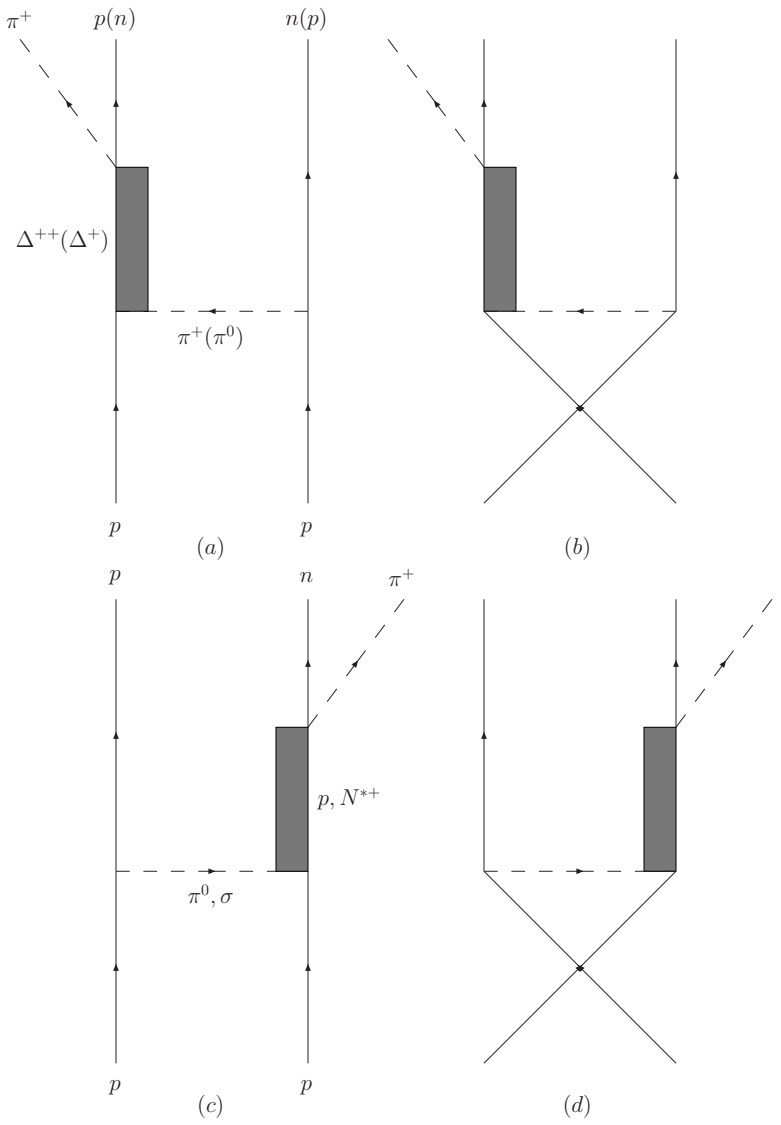

Figure 1:

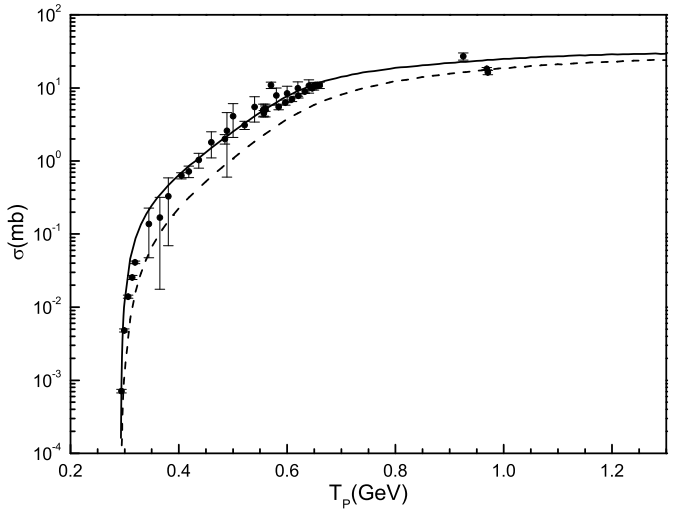

Figure 2:

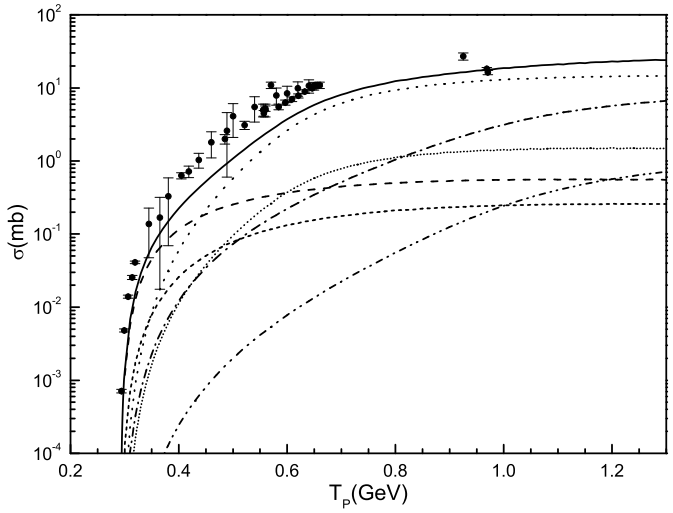

Figure 3:

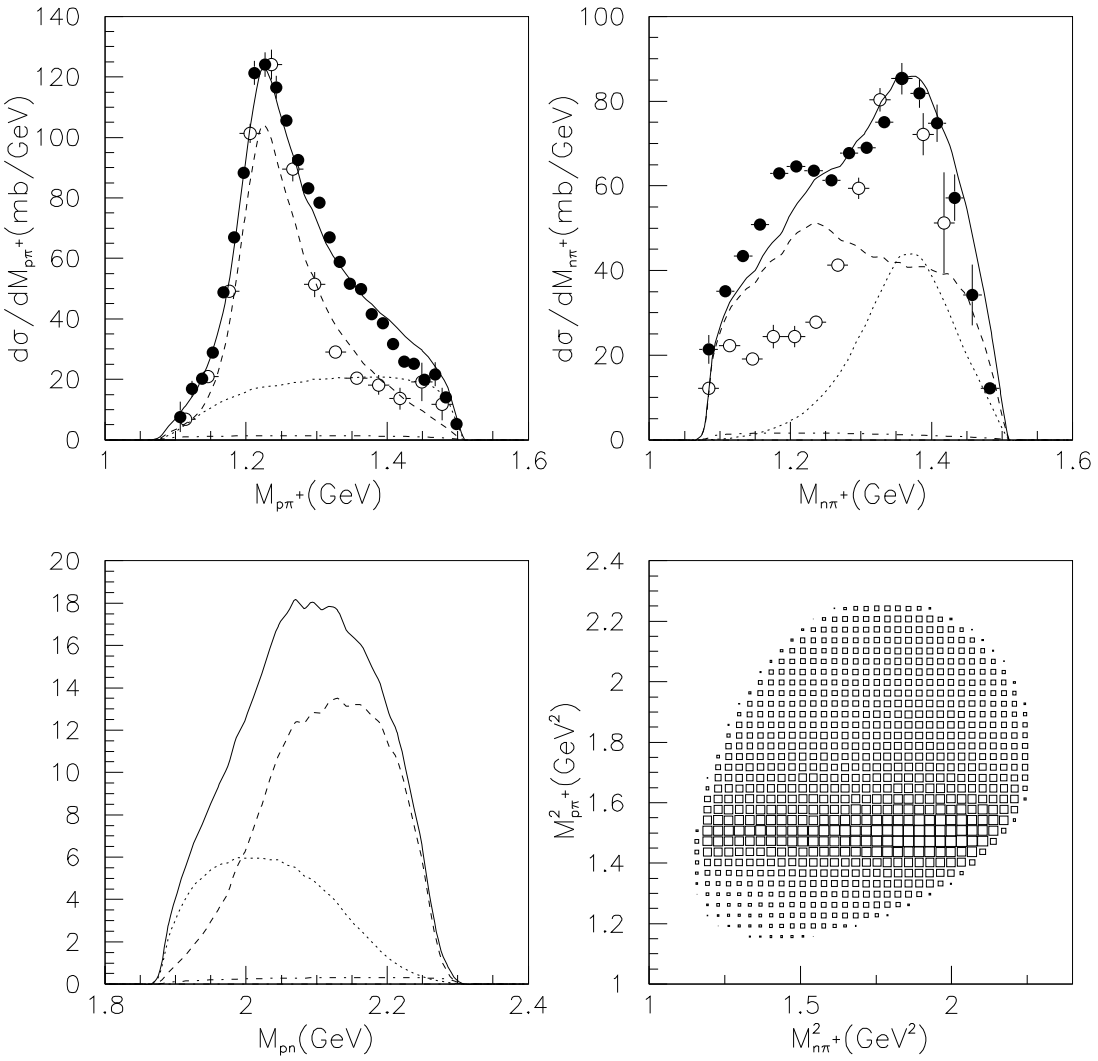
dσ/dM$_{pπ^+}$(mb/GeV)
M$_{pπ^+}$(GeV)
dσ/dM$_{nπ^+}$(mb/GeV)
M$_{nπ^+}$(GeV)
M$_{pn}$(GeV)
M$^2_{pπ^+}$(GeV^2)
M$^2_{nπ^+}$(GeV^2)

Figure 4: